

DOE/BC/15201-2  
(OSTI ID: 782901)

FLUID-ROCK CHARACTERIZATION AND INTERACTIONS IN NMR  
WELL LOGGING

Semi-Annual Report  
August 1, 2000-December 31, 2000

By:  
George J. Hirasaki  
Kishore K. Mohanty

Date Published: July 2001

Work Performed Under Contract No. DE-AC26-99BC15201

Rice University  
Houston, Texas



**National Energy Technology Laboratory  
National Petroleum Technology Office  
U.S. DEPARTMENT OF ENERGY  
Tulsa, Oklahoma**

#### **DISCLAIMER**

This report was prepared as an account of work sponsored by an agency of the United States Government. Neither the United States Government nor any agency thereof, nor any of their employees, makes any warranty, expressed or implied, or assumes any legal liability or responsibility for the accuracy, completeness, or usefulness of any information, apparatus, product, or process disclosed, or represents that its use would not infringe privately owned rights. Reference herein to any specific commercial product, process, or service by trade name, trademark, manufacturer, or otherwise does not necessarily constitute or imply its endorsement, recommendation, or favoring by the United States Government or any agency thereof. The views and opinions of authors expressed herein do not necessarily state or reflect those of the United States Government.

This report has been reproduced directly from the best available copy.

Fluid-Rock Characterization and Interactions in NMR Well Logging

By  
George J. Hirasaki  
Kishore K. Mohanty

July 2001

Work Performed Under Contract DE-AC26-99BC15201

Prepared for  
U.S. Department of Energy  
Assistant Secretary for Fossil Energy

Ginny Weyland, Project Manager  
National Petroleum Technology Office  
P.O. Box 3628  
Tulsa, OK 74101

Prepared by  
Rice University  
6100 Main Street  
Houston, TX 77005-1892

Subcontractor  
University of Houston  
4800 Calhoun Road  
Houston, TX 77204-4792

## TABLE OF CONTENTS

Abstract .....	v
TASK 1: FLUID PROPERTIES .....	1
NMR Properties of Ethane and Propane.....	1
NMR Analysis of Crude Oils .....	3
TASK 2: FLUID-ROCK INTERACTIONS .....	4
Internal Field Gradient.....	4
DOE REPORT – SUB-TASK 3.3 “Study of Vuggy Carbonate Cores Using X-ray CT .....	7
Abstract .....	9
Introduction .....	11
CT Scan Experiments.....	13
Yates Samples .....	14
Flooding Experiment on Chester Field Sample.....	18
Summary .....	28
Acknowledgement.....	28
Reference.....	28

## ABSTRACT

This semi-annual report briefly summarizes the progress since the 1<sup>st</sup> Annual Report issued September, 2000 and the next annual report. More detailed results will be in the annual reports.

The main emphasis on fluid properties was on measurements of the relaxation time and self-diffusion coefficient of ethane and propane. Ethane is similar to methane while propane is more similar to the higher alkanes. The ratio of  $T_1$  and  $T_2$  is demonstrated to be a function of both viscosity and the NMR frequency.

The diffusion-induced  $T_2$  in a uniform magnetic gradient was simulated in one-dimension to seek improved understanding NMR diffusion in restricted geometry. Analytical solutions can be found for this system if the correct region of validity is used.

Estimation of permeability of vuggy carbonates has been problematic because the pore body size does not correlate well with pore throat size. CT scans and CPMG NMR measurements were made on a set of vuggy carbonate rocks.

## TASK 1: FLUID PROPERTIES

### NMR Properties Of Ethane And Propane

The 2000, 1st Annual Report gave the results of methane-alkane systems. Here we report on the NMR relaxation time and self-diffusion coefficient for pure ethane and propane. The  $T_1$  relaxation time for pure ethane and propane are shown on Fig. 1.1 along with the previously reported data. These results show that ethane at ambient and elevated temperature is a super critical fluid and thus is similar to methane. Cryogenic liquid ethane is has a slope similar to that of the higher alkanes but the curve is offset. Liquid propane has only a slight deviation from the trend of the higher alkanes.

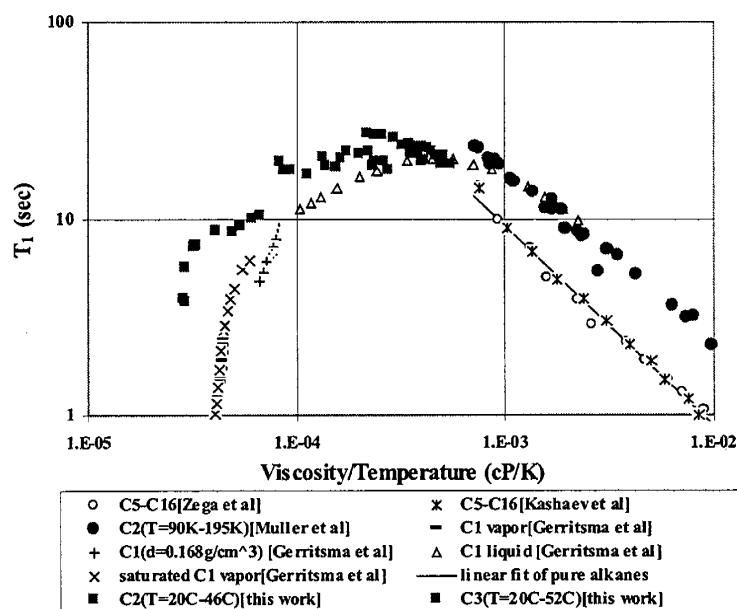


Fig. 1.1 Relaxation time of alkanes as a function of viscosity/temperature

The relaxation time as a function of the self-diffusion coefficient is shown in Fig. 1.2. The liquid alkanes, n-hexane, n-decane, and n-hexadecane have relaxation time that is proportional to the self-diffusion coefficient. Ethane and propane deviate from the linear relationship, similar to the methane-alkane mixtures.

The self-diffusion coefficient is shown as a function of viscosity/temperature in Fig. 1.3. Since these parameters are independent of the NMR relaxation, these parameters have an inverse proportionality, corresponding the Stokes-Einstein relationship.

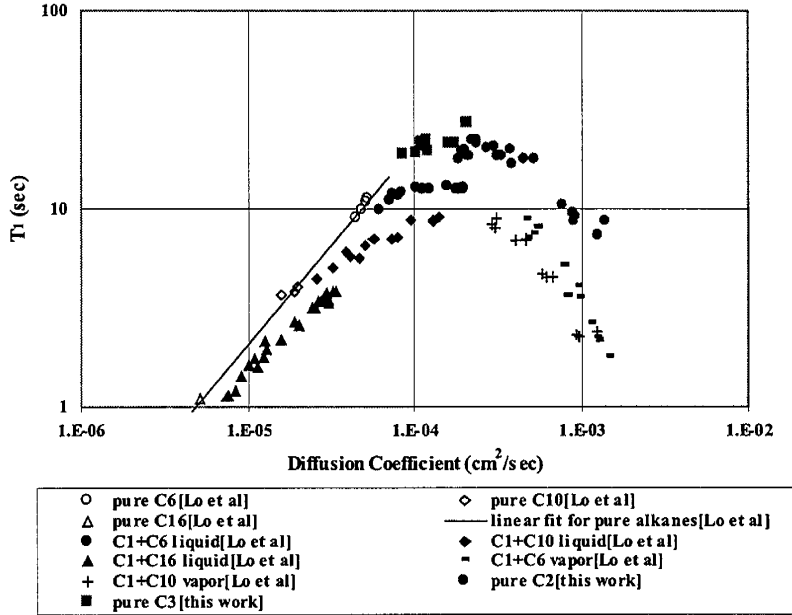


Fig. 1.2 Relaxation time versus self-diffusion coefficient

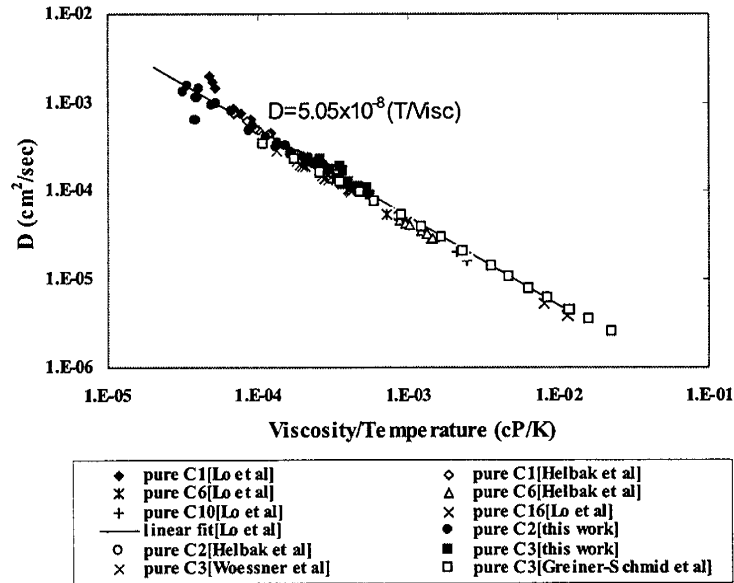


Fig. 1.3 Relaxation time versus viscosity/temperature

Future work will include correlations to describe mixtures as a function of GOR and gas composition.

## NMR Analysis of Crude Oils

It is generally assumed that  $T_1$  and  $T_2$  of crude oils are equal at the NMR frequency of logging tools. However, we observed a systematic difference that appeared to be a function of viscosity. We now see that this difference is also a function of the NMR frequency. Apparently, some of the heavy components of crude oils are not in the "extreme narrowing" condition. This is illustrated in Fig. 1.4. The  $T_1$  is longer than  $T_2$  for viscous oils and more so for 80 MHz compared to 2 MHz.

## $T_1, T_2$ vs. Viscosity for Crude Oils

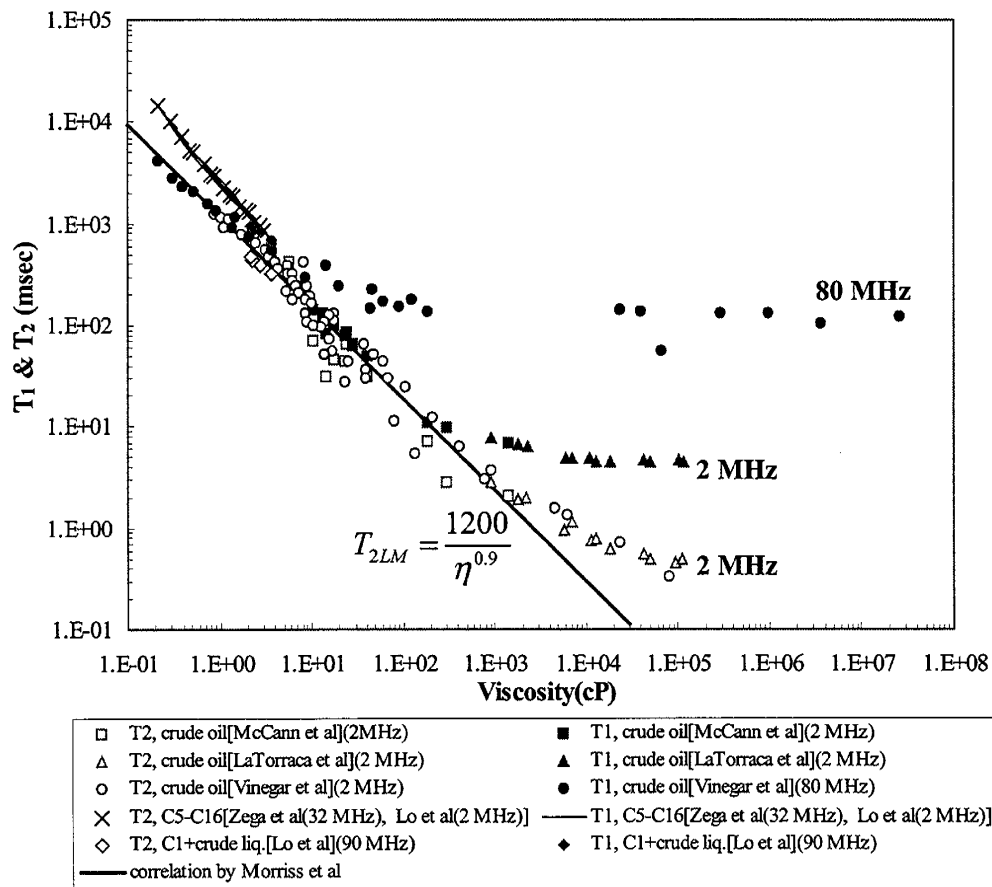


Fig. 1.4  $T_1$  and  $T_2$  relaxation time as a function of viscosity and frequency. The straight line is the correlation for crude oils developed by Morris, et al., (1997)

Future work will include measuring the relaxation time distribution as a function of frequency and developing a correlation dependent on viscosity, temperature, and frequency.

## TASK 2: FLUID-ROCK INTERACTIONS

### Internal Field Gradient

The diffusion-induced  $T_2$  in a uniform magnetic gradient was simulated in one-dimension to seek improved understanding NMR diffusion in restricted geometry. Fig. 2.1 illustrates the dimensionless diffusion-induced  $T_2$  relaxation time as a function of two dimensionless groups.

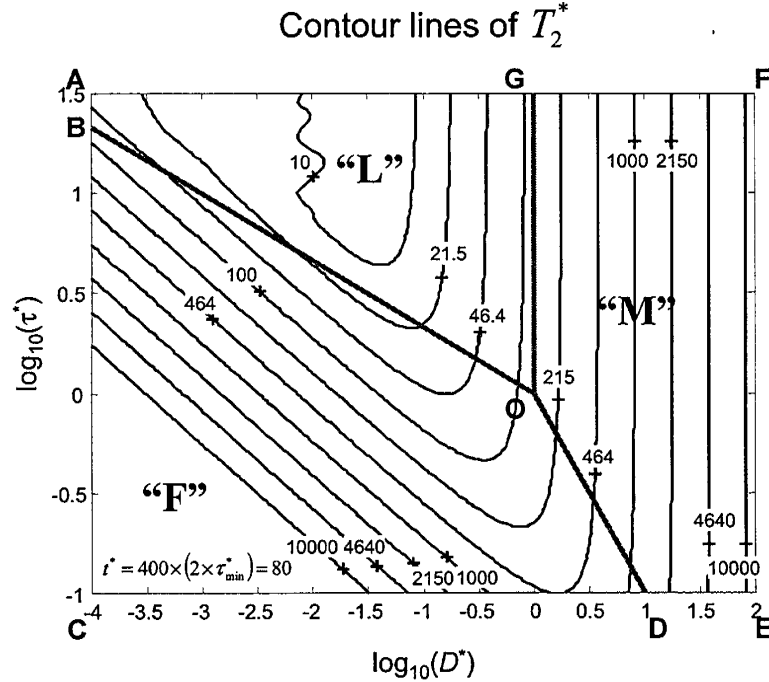


Fig. 2.1 Contour lines of dimensionless diffusion-induced  $T_2$  relaxation time as a function of dimensionless echo spacing and diffusivity.

where

$L_S$ : system length

$L_D = \sqrt{D_0 \tau}$ : diffusion length

$L_g = \left( \frac{D_0}{\gamma g} \right)^{\frac{1}{3}}$ : dephasing length

$T_2^* = T_2 \gamma g L_S$ : dimensionless relaxation time

$D^* = \left( \frac{L_g}{L_S} \right)^3 = \frac{D_0}{\gamma g L_S^3} = \frac{\text{dephasing time}}{\text{diffusion time}}$

$\tau^* = \frac{L_D^2 L_S}{L_g^3} = \tau \gamma g L_S = \text{dimensionless echo spacing}$

The regions in Fig. 2.1 are the "free diffusion regime", "F", the "localization regime", "L", and the "motionally averaging regime", "M". They were identified by deSwiet and Sen (1994) as the region where one length scale is smaller than the other two. The numerical simulation solution appear to change its behavior at different boundaries than those proposed by deSwiet and Sen (1994). We found that by moving the boundaries to those suggested by the numerical solution, the analytical solutions in each of the regions closely match the numerical solution.



**DOE REPORT**  
**SUB-TASK 3.3**

STUDY OF VUGGY CARBONATE CORES  
USING X-RAY CT

I. Hidajat and K. K. Mohanty

Department of Chemical Engineering

University of Houston,

4800 Calhoun

Houston, TX 770204-4792, USA



## **Abstract**

Estimating petrophysical properties of carbonate rocks from NMR measurement is much less reliable than of sandstone. The difficulty arises from the fact that most carbonates exhibit three different length scales from intragranular porosity, intergranular porosity and vugular porosity. The existing permeability correlation from  $T_2$  measurement assumes that vugs do not contribute to permeability, hence a 750 ms cut off is chosen to exclude the vug contribution. This may not always be the case, since vugs may be connected in some formation and contribute to the permeability. The objectives of this work are to identify vug connectivity by using X-ray CT scan, and to improve NMR permeability correlation. CT scanning of dry Yates core material shows that uniformity of vug distribution varies from core to core. CT scanning of core floods in one Chester Field sample shows that the vugs are non-touching. The Chang and Vinegar correlation estimates the permeability correctly from NMR  $T_2$  response because the vugs do not contribute to permeability in this sample. In the future, similar core flood experiments will be performed in some samples from the Yates field.



## Introduction

More than 50% of the world's hydrocarbon reserves is in carbonate formations. However, estimating petrophysical properties from NMR measurements in carbonate rocks have always been a bigger challenge than in sandstone formations. Broad pore size distribution in carbonates, from intragranular porosity to large vugs is the reason for the unreliable estimation of transport properties from NMR logging.

Fig. 1 shows a simplified diagram for classifying different type of pore space in carbonate rocks<sup>1</sup>. The intragranular porosity is the porosity inside the grain ( $\phi_\mu$ ). The intergranular porosity is the pore space between the grains. And the vuggy porosity is defined as the pore space within grains or crystals, or that is significantly larger than grains or crystals.<sup>2</sup> Vugs can be thought of as the absence of one or more grains in packing, or if there is a significant pore space within the grain. The more popular definition for vugs in industry is a pore space that can be easily seen because usually these pores are larger than 200  $\mu\text{m}$  in size.<sup>1</sup>

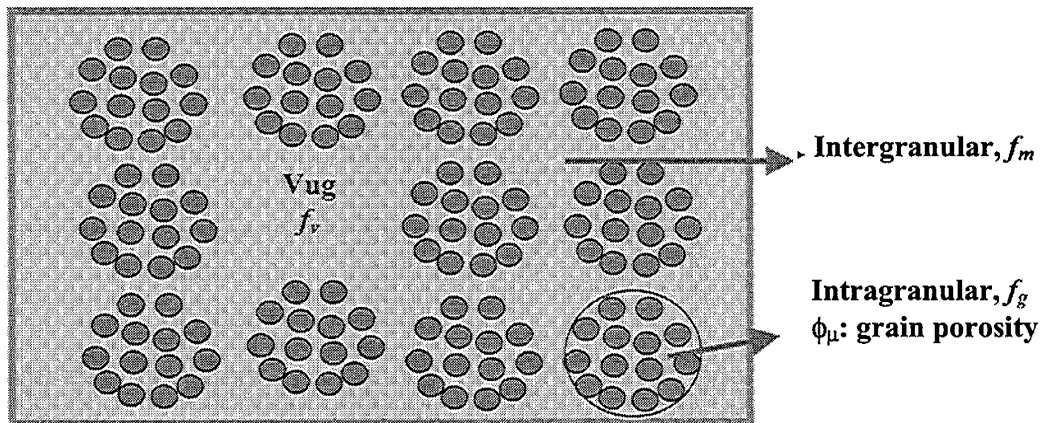


Fig. 1 Simplified Model of Carbonate Rocks

From Fig. 1, we can write:

$$f_v + f_m + f_g = 1 \quad (1)$$

where  $f_v$  is the vug volume fraction,  $f_m$  is the intergranular volume fraction and  $f_g$  is the grain volume fraction. The overall porosity ( $\phi$ ) is given as :

$$\phi = f_v + f_m + f_g \phi_\mu , \quad (2)$$

where  $\phi_\mu$  is the intrinsic porosity of the grain.

Vugs can be classified into separate vugs and touching vugs.<sup>2</sup> Separate vugs are defined as pore space that is interconnected only through the interparticle porosity. Touching vugs are pore space that forms an interconnected pore system independent of the interparticle porosity.

Chang and Vinegar et al. (1997) measured 27 carbonate core plugs and found the permeability correlation from the NMR  $T_2$  distributions as:<sup>3</sup>

$$k = 4.75 (\phi_{\text{NMR}, 750})^4 (T_{2, 750})^2 \quad (3)$$

where  $k$  is the permeability (mD),  $\phi_{\text{NMR}, 750}$  and  $T_{2, 750}$  is the porosity and the logarithmic mean of  $T_2$  distribution with  $T_2 < 750$  ms. The correlation assumes that vugs have  $T_2$  distribution larger than 750 ms and they do not contribute to the permeability. In other words, they assume that all the vugs are separate vugs. This may not be the case, in some instances vugs may be connected and contribute to the permeability.

Hicks (1990) conducted CT Scan study on carbonate rocks from Fenn Big Valley and San Andres (TX) dolomite.<sup>4</sup> He studied the porosity distribution, residual saturations and miscible displacements. However, no study was conducted on the connectivity of the vugs.

The objective of this work is to study the vug connectivity and to improve the permeability correlation from NMR for vugs contribution. From CT Scan experiment, we

can investigate the connectivity and the distribution of the vugs in the rock sample. Other measurements such as: permeability, capillary pressure, Sor and thin section will also be performed. By combining the matrix structure information from the thin section and the vugs distribution from the CT Scan, we will be able to construct a representative porous media and simulate different vugs configuration. Finally, from all the information both from experiment and simulation we may identify the condition where vugs contribute to permeability.

## 2. CT Scan Experiments

CT scanning is done by using a Deltascan 2060HR CT scanner manufactured by Technicare Corporation. The scanner gantry has been rotated 90° from the conventional vertical position so that the scan plane is horizontal. This enables the fluid displacements to be conducted in the vertical direction. The scanner resolution is 0.25 x 0.25 x 2mm for each voxel. All experiments reported here were conducted with the scan plane horizontal. For flow experiments, a core is put into a hassler type core holder. The core holder is mounted on a table positioned below the gantry and the table is raised or lowered to place the core at the desired position. The position of the core can be reproduced to within 5 µm in the vertical direction. During a scan, the X-ray source rotates through a full circle in the scan plane around the core sample. The 720 detectors located around the scan circle detect the X-ray signal, then the host computer will process the data and perform a reconstruction. The reconstructed image is a matrix of 512 x 512 pixels, and each pixel represents the voxel size as described above. Table 1 shows the available parameters in the CT scan and the selected parameters for the entire experiments done.

Parameter	Available	Selected
Voltage (KV)	80, 100, 120	120
Current (mA)	25, 50, 75, 100	75
Scan time (sec)	2, 4, 8	8
Scan diameter (cm)	12, 25, 40, 50	12
Slice thickness (mm)	2, 5, 20	2

Table 1. Available and Selected Parameter in CT-Scan

The first CT experiment was done on Yates samples. The samples were directly scanned without putting them into the coreholder. No flow experiment was done at this stage. The purpose was to study the sample structure and identify suitable positions for plugging 1” or 1.5” core samples.

The second CT experiment was done on a Chester Field sample and involved flooding experiments. The purpose of the experiment is to investigate the porosity distribution, preferential flow path, and oil saturation at  $S_{wr}$  and at  $S_{or}$ .

### **3. Yates Samples**

Six Yates bare samples are scanned, and we present three of them since the other three can be categorized into these three classes. The scans were taken at 1-cm interval.

The first sample is 17C9; the sample is 6 cm in diameter and 6.8 cm in height. The sample is not cylindrical. The picture of the sample is shown in Fig. 2. Visually it is observed that the matrix is very tight and there are a lot of vugs; the vug size is about 1 mm to 3 mm. Vugs are distributed more or less uniformly throughout the sample (Fig. 3). Small diameter plugs are representative of the medium.

The second sample is 2416; the sample is 7 cm in diameter and 10.6 cm in height. The matrix also looks very tight and vugs are not uniformly distributed. Fig. 4 shows the picture of the sample. Vugs occur only in some layers, and the other layers there are almost free of vugs, as indicated in CT images (Fig. 5). Most of the vugs are small and less than 0.5 mm. A few vugs have size about 1 mm.

The third sample is 7626B; the sample is 8 cm in diameter and 17.9 cm in height. The matrix looks permeable, but the vugs distribution is not uniform. Fig. 6 shows the picture of this sample, which has some large vugs with size up to 5mm. The small vugs are scattered throughout the sample with size about 1mm – 2mm. The CT images are given in Fig. 7.

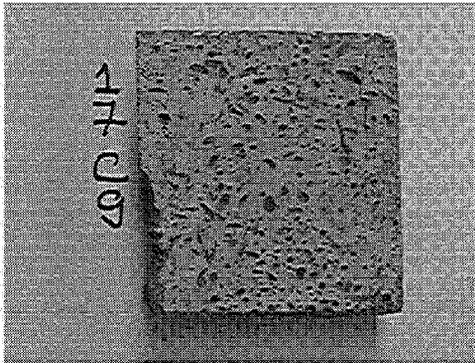
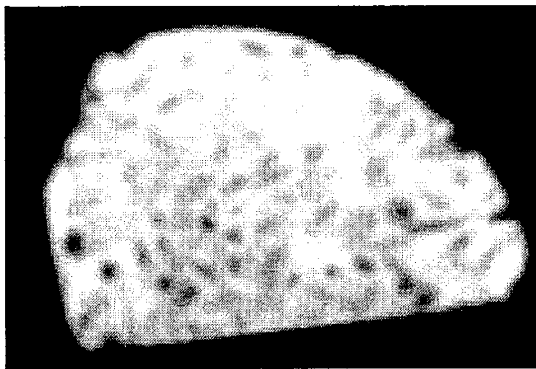
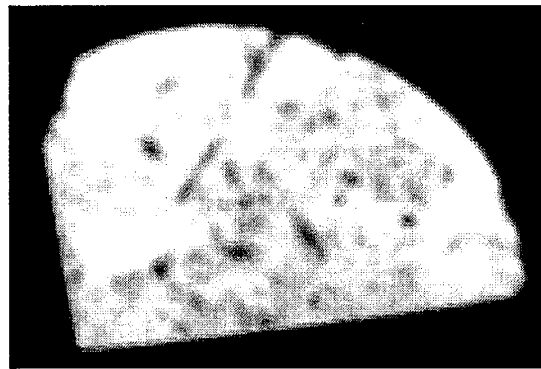


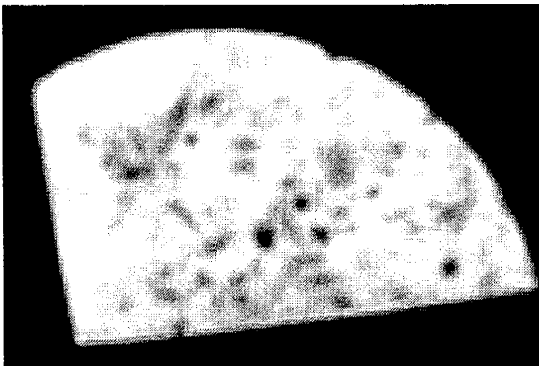
Fig. 2. Picture of sample no.17C9



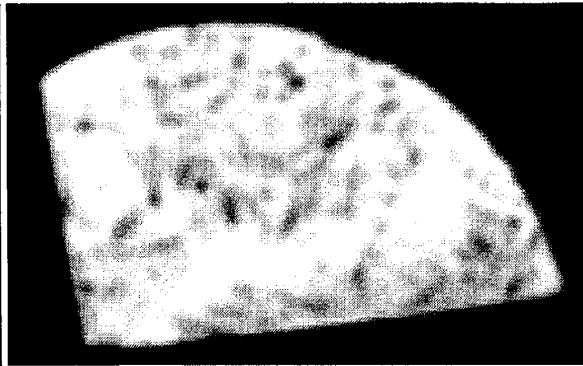
Slice 1



Slice 3



Slice 5



Slice 8

Fig. 3 CT Image for sample 17C9 at selected slices

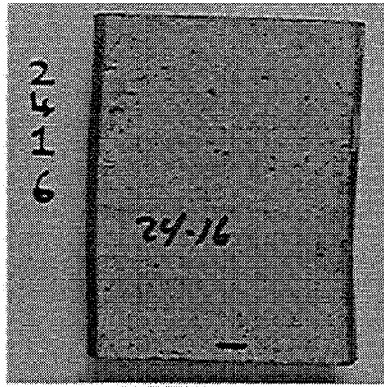
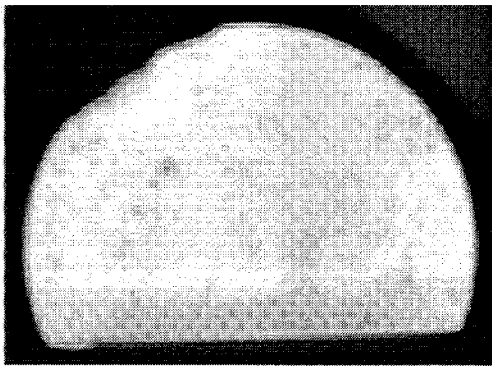
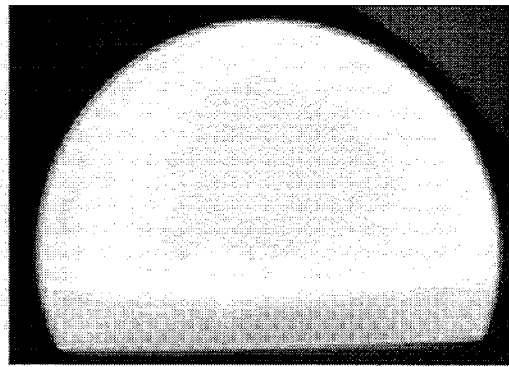


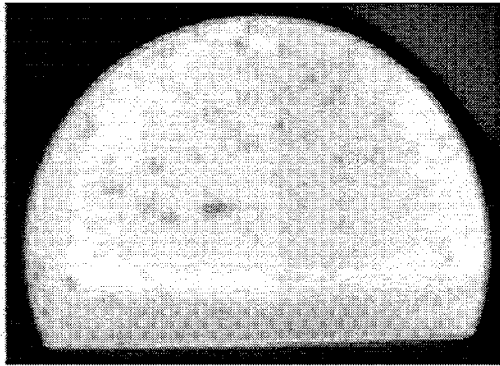
Fig. 4 Picture of sample no. 2416



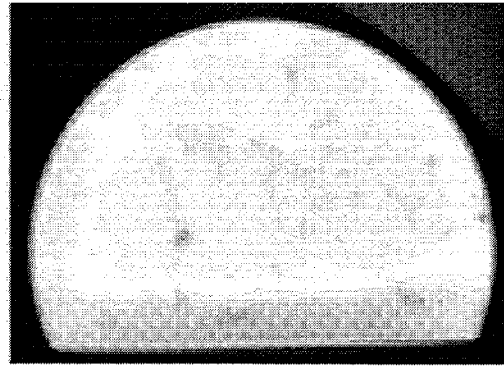
Slice 1



Slice 4



Slice 7



Slice 10

Fig. 5 CT Images for Sample 2416 at selected slices

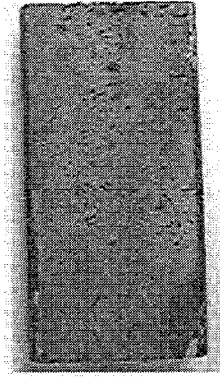
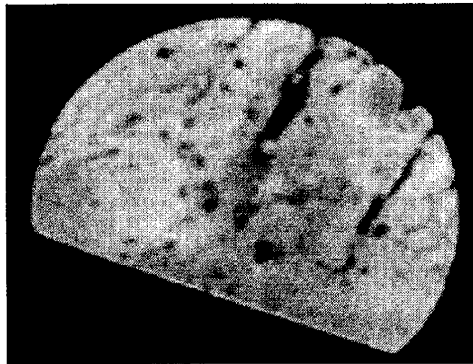
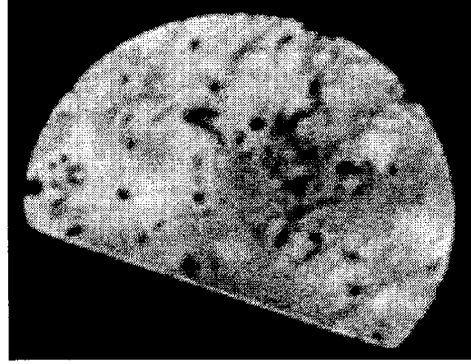


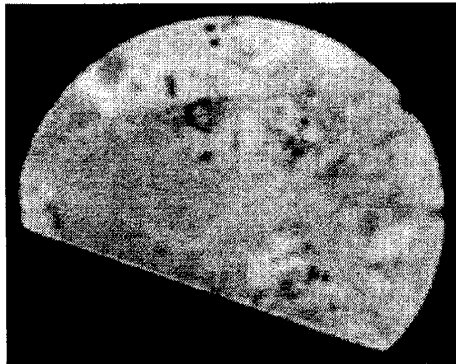
Fig. 6 Picture of sample no. 7626B



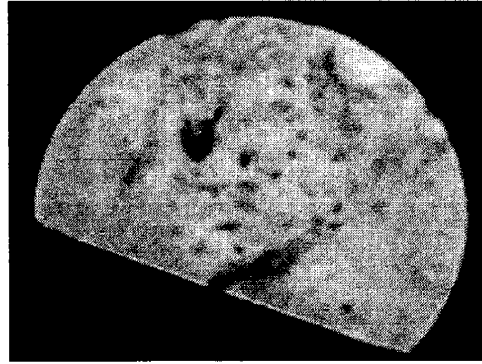
Slice 4



Slice 6



Slice 11



Slice 15

Fig. 7 CT Images for Sample 7626B at selected slices

#### 4. Flooding Experiment on Chester Field Sample

The second experiment is performed on the Chester Field sample. This plug is a dolomite, 1" in diameter and 1.5" long. According to the data from Shell, the porosity is 17.8% and the air permeability is 115 mD. The calculated pore volume from the porosity is 3.6 ml. Vugs of about 1 – 2 mm are visible on the plug. The sample was put into a core holder and an overburden pressure about 700 psi was applied. The scans were taken at 4-mm interval. Doped brine and doped oil are used in some experiments to increase the image contrast.

The following experiments were conducted on this sample:

1. The core was scanned in vacuum condition.
2. The core was saturated with brine (1 wt% of NaCl), and scanned. By subtracting with the CT image taken in step 1, porosity distribution of the core was obtained.
3. The core was flooded with doped brine (15 wt% of NaI in brine) and scanned at different time. From this step, preferential flow path was investigated.
4. The core was flushed with brine and scanned.
5. The core was flooded with doped oil (15 wt% of Iododecane in n-decane) until  $S_{wr}$  was reached and scanned to obtain oil distribution at  $S_{wr}$ .
6. The core was flooded with brine until  $S_{or}$  was reached and scanned to obtain oil distribution at  $S_{or}$ .
7. The core was taken out from the coreholder. NMR  $T_2$  response was measured at  $S_{or}$  condition.
8. The core was cleaned by using Dean-Stark extraction apparatus. Toluene was used as the cleaning fluid. The amount of water collected was measured.
9. The core was resaturated with brine and NMR  $T_2$  response was measured at 100% brine condition.

The porosity distribution from the CT Scan for each slice is given in Fig. 8. The light colored area indicates high porosity region. The high porosity regions are uniformly distributed in slices 1 through 6; they shift towards the upper right area in slices 7 -10.

Each slice contains a few vugs (from one vug to about four vugs) and the vugs appear not to be touching.

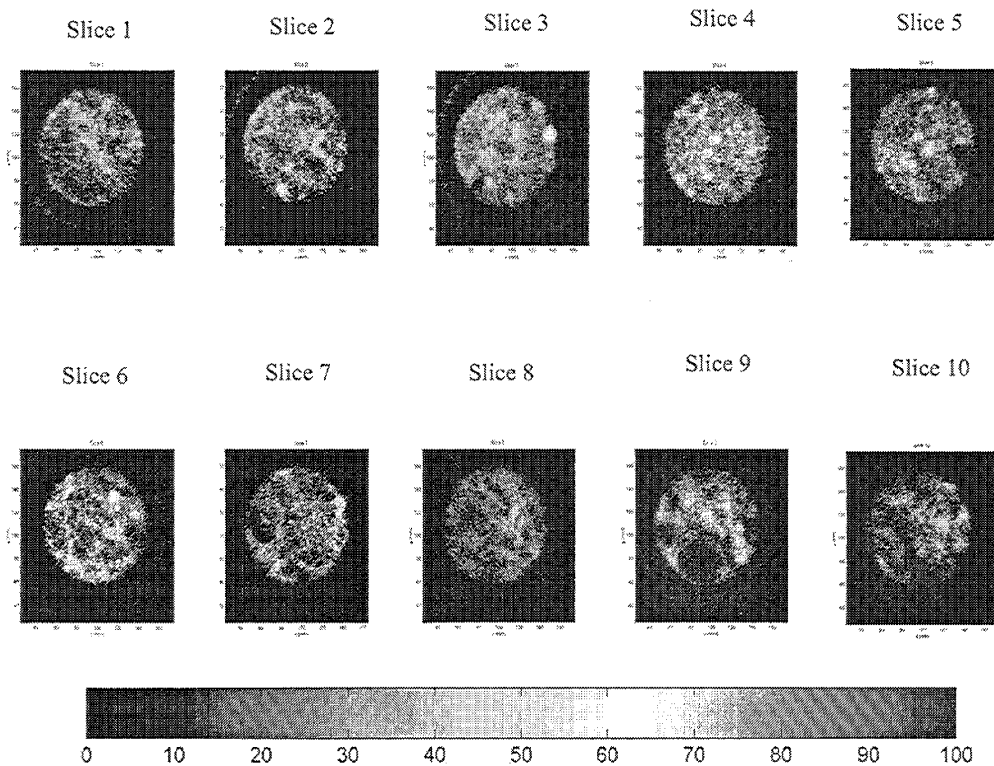
Figs. 9 through 11 show the doped brine profile at 0.25, 0.5 and 1.25 injected pore volume, respectively. Note that the color represents the CT number difference between the core with doped brine and the core in vacuum condition, and it is not actual doped brine concentration. Because of the machine problem during the experiment, we were not able to take scan of the fully saturated core at 100% doped brine saturation at the same scan condition. The CT number difference reflects the concentration of doped brine in the core. At 0.25 PV injected, the brine had not reached slices 7 through 10. The doped brine flowed through high porosity area, and clearly some vugs in slice 1, 2, 3 and 6 were in this flow path. At 0.5 PV injected, the brine breakthrough had occurred. As shown in Fig. 10, there were vugs in slices 9 and 10 in this flow path. Similar to the porosity distribution, the flow path moved to the upper right past the slice 7. There were some vugs in slice 9 that had not been invaded by doped brine yet, indicating that those vugs were not in the preferential flow path and channeling occurred. At 1.25 PV injected, most of the pore space was invaded by doped brine. The vugs are indicated with very light color region. This experiment shows that although the vugs are not touching, most of them are in the preferential flow path.

Fig. 12 shows the doped oil distribution at irreducible water saturation ( $S_{wr}$ ) condition. The calculated  $S_{wr}$  from the material balance is 52%. The data for slice 1 is corrupted and it is not shown. Again, the color refers to the CT number difference between the core with doped oil and the core with saturated brine. To obtain the doped oil saturation profile, scan from 100% doped oil saturated core is needed which is not available at this stage. The CT number difference, again, reflects the amount of doped oil. From the CT images in Fig. 12, the doped oil appears to be almost uniformly distributed in the high porosity area. All the vugs are occupied by the oil.

Fig. 13 shows the doped oil profile at the residual oil saturation ( $S_{or}$ ) condition. The computed  $S_{or}$  from the material balance is 32%. Again, the color refers to the CT number

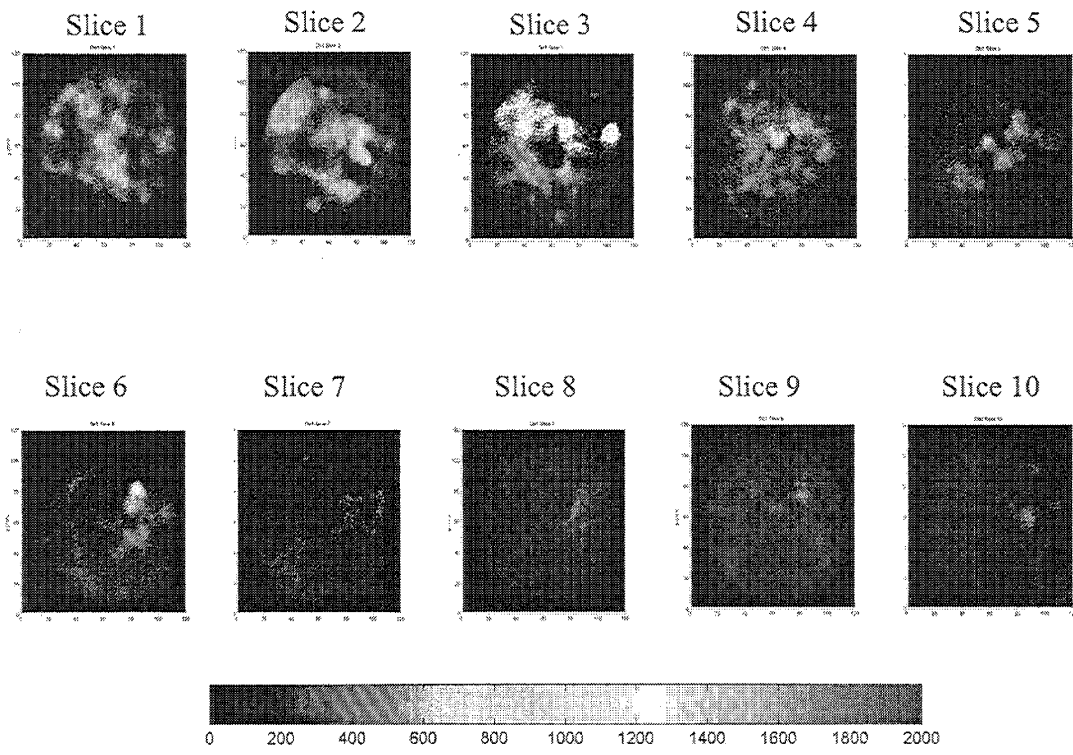
difference between the core with doped oil and the core with saturated brine. From the CT images in Fig. 13, the doped oil is mostly swept from the middle region of the core, and the  $S_{or}$  resides in the perimeter region. The pore volume computed from the Dean Stark extraction is 3.67 ml, which is consistent with the pore volume calculated from the porosity data from Shell.

$T_2$  distributions at  $S_{or}$  and 100% brine saturation are shown in Fig. 14. The solid line represents the  $T_2$  distribution at 100% brine saturated. The peak occurs at 600 ms and the computed  $T_{2logmean}$  is 381 ms. There is a significant region at  $T_2$  greater than 750 ms, indicating the presence of vugs. The computed permeability from Eq. 3 is 99 mD, which agrees well with the air permeability. This also confirms that vugs are non-touching and do not contribute to its permeability. The dashed line in Fig. 14 shows the  $T_2$  distribution for the doped oil. The main peak is at 500 ms and the response is bimodal because the oil is not pure n-decane. The dotted line represents the  $T_2$  distribution for the core at  $S_{or}$ . This  $T_2$  distribution is very similar to that for brine saturated core. The similarity in  $T_2$  distribution greater than 750 ms indicates that the vugs are filled with brine. This is unlike the common assumption that residual oil occupies the vugs in water wet media.



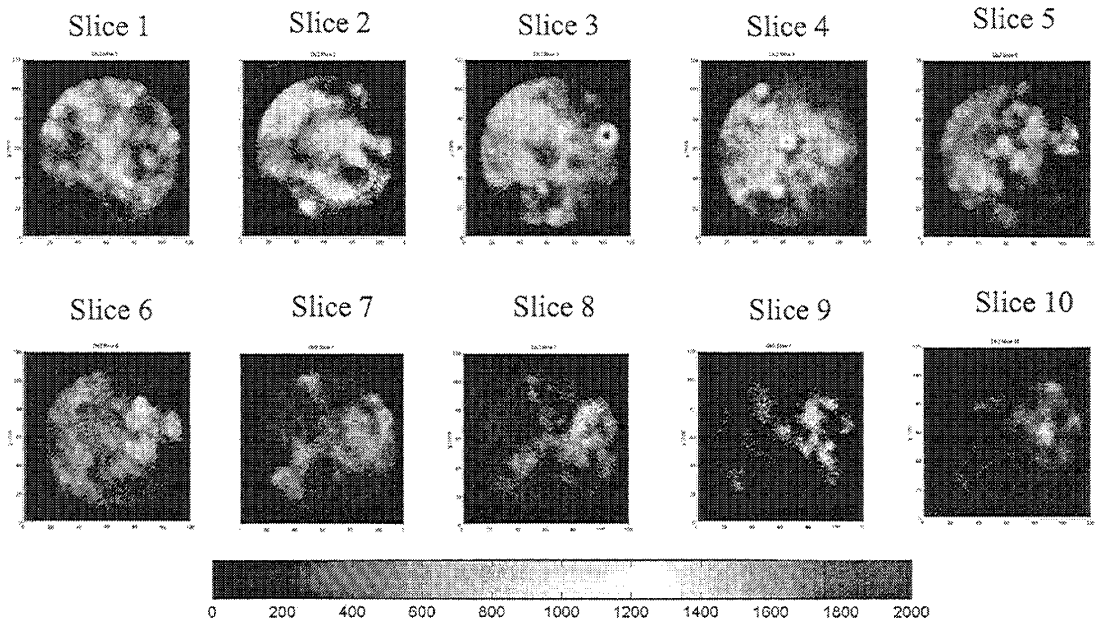
Porosity %

Fig. 8 Porosity Distribution from CT Scan



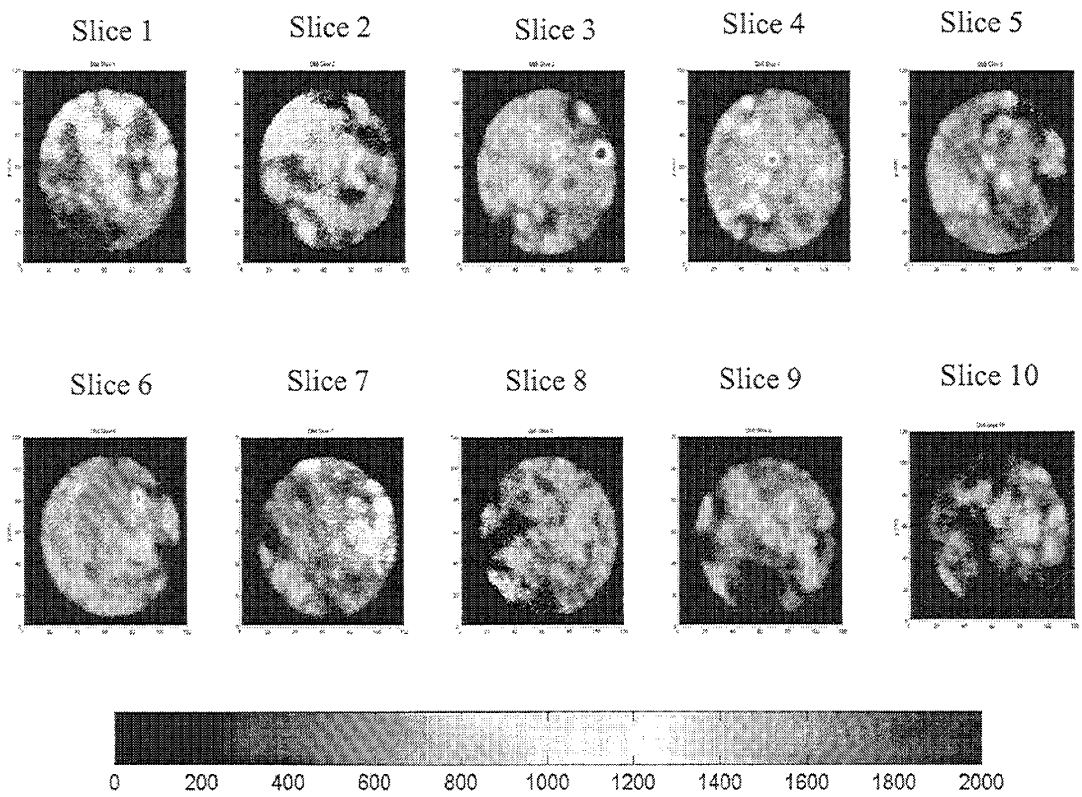
CT Number

Fig. 9 Doped brine profile at 0.25 PV Injected



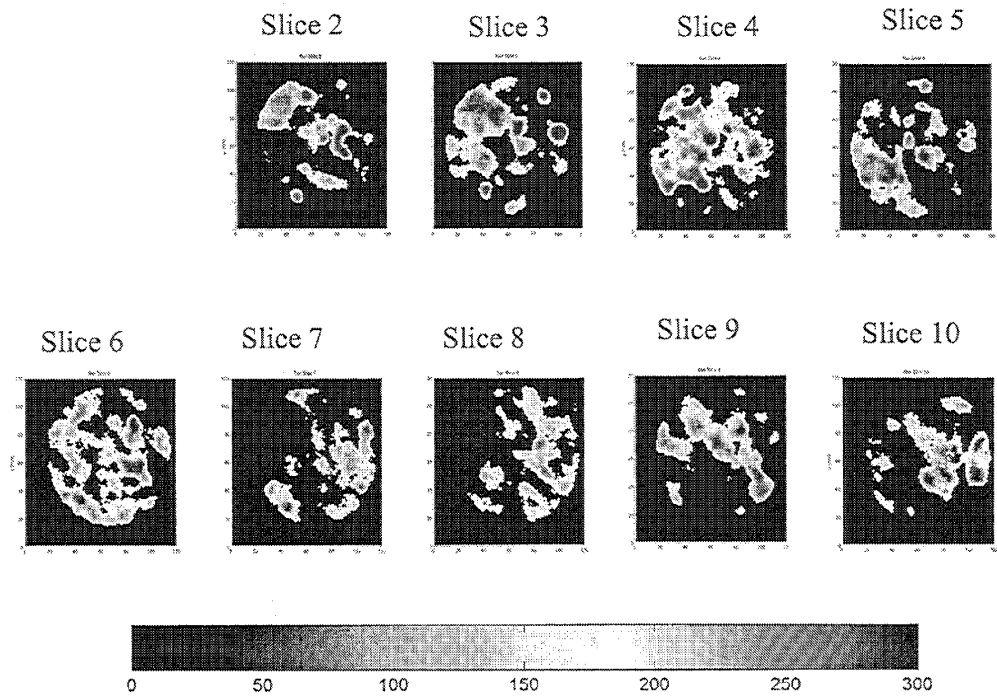
CT Number

Fig. 10 Doped brine profile at 0.5 PV Injected



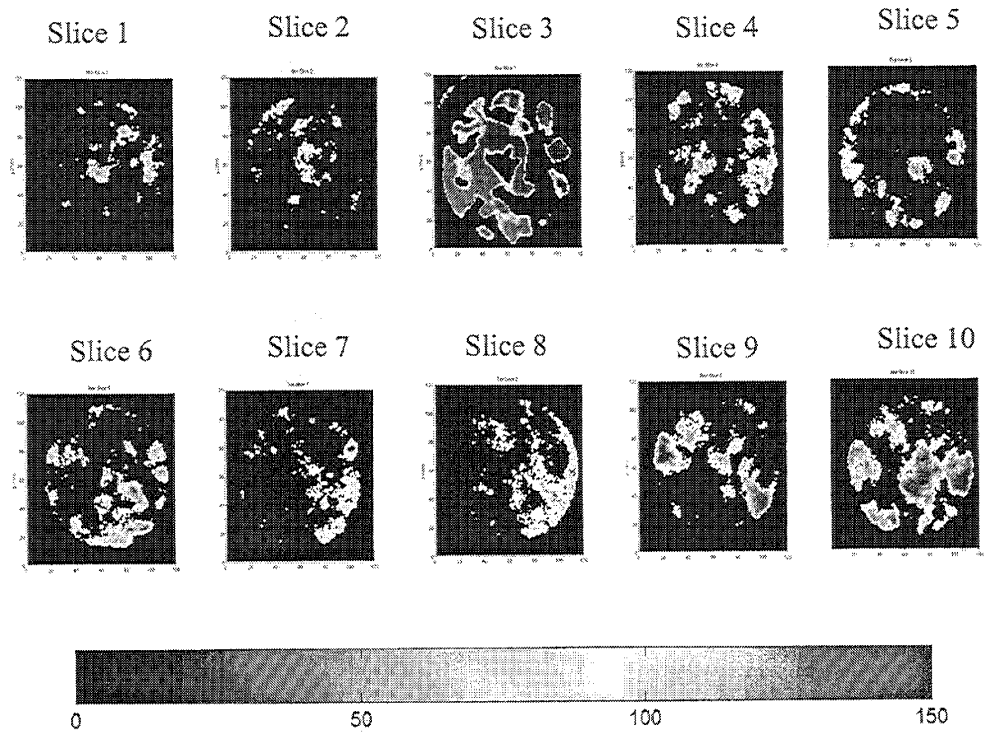
CT Number

Fig. 11 Doped brine profile at 1.25 PV injected



CT Number

Fig. 12 Doped Oil Profile at  $S_{wr}$



CT Number

Fig. 13 Doped Oil Profile at  $S_{or}$

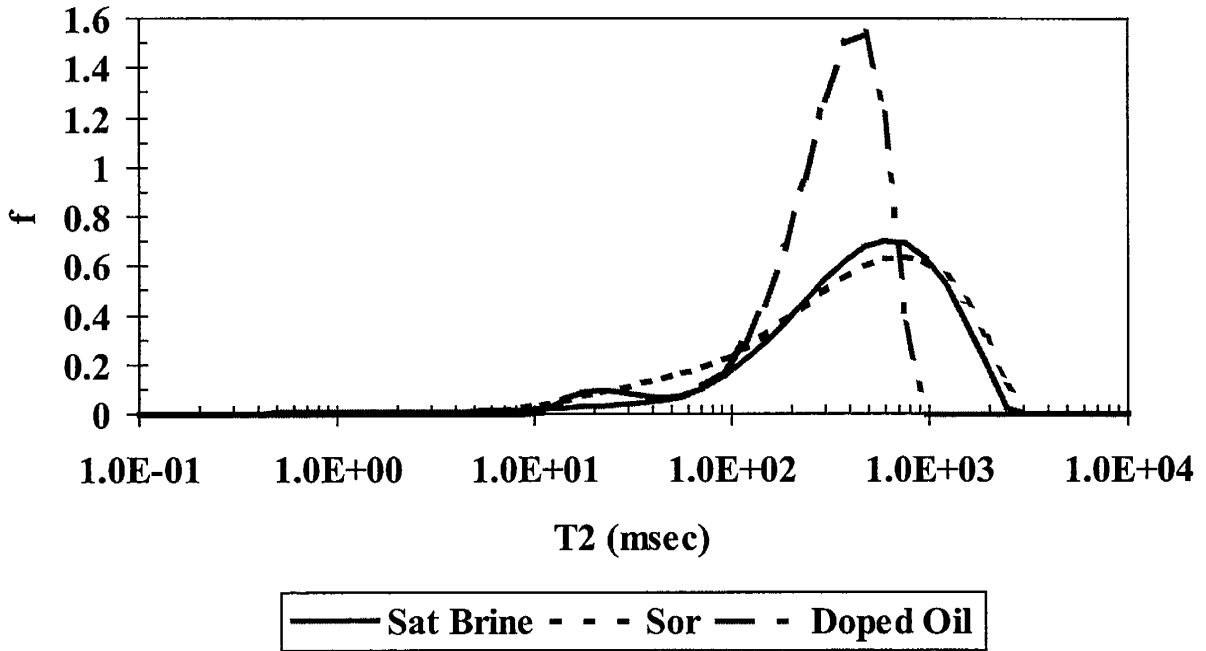


Fig 14. T<sub>2</sub> distribution for Chester Field sample and for doped oil

## **Summary**

This work has demonstrated the use of X-ray CT scanning for studying porosity distribution, vugs distribution, preferential flow path and oil distribution at  $S_{wr}$  and  $S_{or}$  for core samples. CT scanning of dry Yates core material shows that uniformity of vug distribution varies from core to core. CT scanning of core floods in one Chester Field sample shows that the vugs are non-touching. The Chang and Vinegar correlation estimates the permeability correctly from NMR  $T_2$  response because the vugs do not contribute to permeability in this sample. In the next six months, similar core flood experiments will be performed in some samples from the Yates field.

## **Acknowledgment**

We would like to thank Marathon Oil Company and Shell Development Company for providing the carbonate samples.

## **Reference:**

1. T.S. Ramakrishnan, A. Rabaute, E. J. Fordham, R. Ramamoorthy, M. Herron, A. Matteson, B. Raghuraman, A. Mahdi, M. Akbar and F. Kuchuk, "A Petrophysical and Petrographic Study of Carbonate Cores from Thamama formation", SPE 49502, 1998.
2. F. J. Lucia, "Carbonate Reservoir Characterization", Springer, New York, 1999.
3. D. Chang, H. Vinegar, C. Morriss, and C. Straley, "Effective Porosity, Producing Fluid, and Permeability in Carbonates from NMR Logging", The Log Analyst, 1997.
4. P. J. Hicks, Jr., "A Study of Heterogeneous Carbonate Cores Using X-Ray CT: Porosity, Residual Saturations and Miscible Displacements", Ph.D. Thesis, University of Houston, 1990.

